Uniqueness Of Refractive Index As An Effective Diagnostic Parameter For Brain Lesions: A Novel Noninvasive Technique To Predict Refractive Index From CT-MR Fusion Image By Applying Feynman's Equation

T Biswas, S Ramadan, S Ghosh, R Bhattacharya

Citation

T Biswas, S Ramadan, S Ghosh, R Bhattacharya. *Uniqueness Of Refractive Index As An Effective Diagnostic Parameter For Brain Lesions: A Novel Noninvasive Technique To Predict Refractive Index From CT-MR Fusion Image By Applying Feynman's Equation*. The Internet Journal of Radiology. 2012 Volume 14 Number 1.

Abstract

PURPOSE – The refractive index (RI) is a unique physical property of tissue. It changes in neoplastic and inflammatory condition of brain due to depletion of tissue glutathione concentration changing the electron density. The purpose of the study was to predict RI value of the brain lesions from the CT-MR fused images non invasively. MATERIALS AND METHODS –CT-MR fusion image was produced by combining CT and MR images by rigid registration technique to detect the pathology accurately. Independent component analysis determines the color value and gray value of the images of the tissue. These values were then used by Neural Network software to generate a color mapping of the CT-MR fusion image. Electron density derived from CT images and optical frequency from color image were used to determine RI value by applying Feynman's equation. RI value and glutathione levels of corresponding biopsy specimens were determined in the laboratory. RESULTS –.A colored CT-MR fusion image shows true color of the tissue. The RI values determined from images were in agreement with biopsy determined RI values. Values between 1.353 through 1.359 are benign and RI value above 1.412 were found malignant.CONCLUSION- Predicting RI value using colored CT-MR fused images will increase diagnostic accuracy.

INTRODUCTION

Accurate diagnosis of tumors and other brain lesions can not be done by conventional MR imaging alone. Even other additive MR tools such as spectroscopy (MRS) and diffusion weighted imaging (DWI) sometimes fail to differentiate between tumor and a pseudo tumoral lesions like tumefactive multiple sclerosis(1). In some cases lymphoma and metastasis are difficult to discriminate by MR Spectroscopy also (2). This study aims to evaluate the potential usefulness and the added value that RI value could provide to this discrimination.

The refractive index is one of the important physical parameters in biomedical diagnostics. Using a rigid registration technique, CT and MRI images can be fused together to generate one CT-MR fused image, which can be colorized by Neural network software to generate true-color CT-MR fused image of the brain, thus highlighting pathology. RI value can be predicted from (i) the electron density of CT images and (ii) the optical frequencies of the color of the lesion and normal brain tissues. The in situ RI value of naturally colored tissue in vivo and in vitro can serve as an important indicator of tissue state. We describe a novel approach to predict RI from CT-MR fused images by applying Feynman's equation described in the Physics basis of RI.

BIOLOGICAL BASIS OF THE REFRACTIVE INDEX

RI is dependent on the interaction between electromagnetic waves and tissue. The scattering properties, color and image quality depend on the differences in RI among the components of the tissue (3). In disease states, such as neoplasm or inflammation, color of tissue changes due to the change in RI, which in turn is related to the dielectric constant (ε_r) or relative permittivity of the tissue (4). The dielectric constant changes as a result of changes in electron density of the tissue. The electron density of the tissue changes due to the derangement of the electron transport system of the inner mitochondrial membrane (5). Several

studies have demonstrated that cells exposed to hypoxic conditions (1.5% O_2) produce increased levels of reactive O_2 species (ROS) derived from the mitochondrial electron transport chain (mt ROS). The generation of mt ROS under hypoxia is likely to alter intracellular redox status and glutathione (GSH) levels (6).

The role of oxidative stress in the genesis of various types of tumors, particularly in malignancy, is well-established. Several chemical, cell culture, and animal studies indicate that antioxidants such as GSH may slow or even prevent the development of malignant tumors (7). The brain is considered abnormally sensitive to oxidative damage, since brain tissue has a high rate of oxygen consumption, high lipid content, and relatively low antioxidant defense, compared to other tissues. GSH is a tripeptide (L glutamyl Lcysteinyl glycine) and a potent antioxidant (8). Selenium-dependent glutathione peroxidase (GPx) plays a protective role in oxidative stress-induced apoptosis.

Particularly with the help of menadione (VitK3), it is believed that GPx activates the electron transport system and increases intracellular superoxide radicals (9). In the white matter of

normal brain tissue, the GSH content is 1.2+0.15 mM (910)). An increase in GSH levels is found in meningioma (1.5 to 3mM) (11). However diminished amounts of GSH are found in gliomas and astrocytomas (0.78 to 1 mM). It is found the degree of malignancy is inversely proportional to GSH levels. GSH is important in maintaining a normal value of RI, as shown in the lens of the eye (12). Normal RI value of gray matter is 1.395 and that of white matter is 1.412 (13). In our study we have found that tissues whose RI value deviated from the above normal values were found to be abnormal. Thus, in vivo measurements of the RI of a brain lesion may replace the hazards of stereotactic biopsy.

RI is related to the dielectric constant of tissue, which in turn depends upon electron density (ED) of the tissue and wavelength or optical frequency (f) of its color (14). We have developed a novel, noninvasive in vivo technique to determine in human the RI value of gray matter, white matter, brain tumors, and other brain lesions from colored CT-MR fusion images. Using image registration and histogram-matching techniques, computer-generated color images can be produced from the MRI (15). MR images are superior to CT images in showing anatomical features, while CT provides important information about the electron density of the tissue. CT Number is also incorporated in the calculation of CT-MR fusion image pixel by registration technique. The incorporation of data of multiple image modalities offers the potential to improve diagnosis. This multi-parametric approach is explained in the image processing section.

PHYSICS OF THE REFRACTIVE INDEX

According to Richard Feynman (16), RI can be calculated using the following equation:

Where,

Figure 1

$$RI = 1 + \frac{ED \times e^2}{2\varepsilon_0 m(\omega_0^2 - \omega^2)}$$

$^{>2}$ = $4\pi 2f^2$ (Hz^2)

f = optical frequency (Hz)

=angular frequency of the electromagnetic radiation = $2\pi f$ (Hz)

ED = Electron density (number of electrons per unit volume of the material /m^3)

e= Charge of electron =$1.602X10^{-19}$ coulomb (c),

m=mass of electron = $9.10938188 \times 10^{-31}$ kg,

= dielectric constant in relation to vacuum = $8.85X10^{-12}c^2s^2/kgm^3$

= resonant frequency of an electron bound in an atom of the tissue =3.74×10^{16} Hz.

The altered RI value of a tumor or lesion can be mathematically predicted from different datasets, such as the electron density of the lesion, derived from the CT Number of the image pixel, and optical frequency, determined by the color of the lesion. From the predicted RI value, the dielectric constant of the tissue ($_r$) can also be calculated, which is the square of RI value ($_r=RI^2$)

Relationship of refractive index to mass density of tissue (RI–density relationship) and consistency of the tissue are

also important. Combined empirical and laboratory analyses show that a denser material (tissue) generally tends to have a larger RI because the applied electric field induces a greater number of electric dipoles, and that the RI–density relationship can be described reasonably well by the Lorentz–Lorenz relation (17).

MATERIALS AND METHOD

CT and MR imaging data were collected from normal brain as well as from the pathological cases. After obtaining proper institutional ethics, 81 normal control cases and 32 pathological cases were studied. Pathological cases included low grade glioma, pilocytic astrocytoma, glioblastoma, low grade oligodendroglioma (gradeII) , solid brain abscess, tumefactive multiple sclerosis, lymphoma, metastasis from breast and lung cancer and post fossa lesions, such as medulloblastoma (Table1).

Figure 2

TABLE-1.Type and Number of Pathological Cases

Tissue	Number of cases
GLIOMA	**25**
Low grade glioma	6
Glioblastoma	14
Oligodendroglioma-	2
Pilocytic Astocytoma--	1
Medulloblastoma--------	2
INFLAMMATORY-	**3**
Tumefactive MS	2
Solid brain abscess	1
OTHERS	
Metastasis	2
Lymphoma-	2

Each patient underwent CT scan and MRI. Single voxel MR Spectroscopy of ipsilateral and contralateral side was performed especially on patients with brain lesions to know the underlying pathology.. Biopsy specimens of the post-surgical patients were sent for histopathology and for determination of RI by refractometer and ellipsometer.

DETERMINATION OF ELECTRON DENSITY FROM CT NUMBER

CT Number is the ratio of difference of linear attenuation coefficients of tissue (s) and water (w) to the linear attenuation coefficient of water multiplied by 1000; thus:

Figure 3

$$\text{CT NUMBER} = \frac{\mu s - \mu w}{\mu w} X1000 \quad \text{Hounsfield (HU) Unit}$$

The linear attenuation coefficient of a material describes the fraction of a beam of x-rays or gamma rays that is absorbed or scattered per unit thickness of the material.

The linear attenuation coefficient depends on the photon energy, chemical composition and physical density of the material (18).

The CT Numbers for normal brain tissue, as well as for various brain tumors and lesions, were determined in a conventional third generation CT scanner (Wipro-GE, India, Sytec 1800i). These CT Number values were compared with the gray value of the CT images, using a matrix size of 512 × 512, an in plane resolution of 0.5 mm, and a slice thickness of 5 mm. ED of normal and abnormal gray white matter were determined using standard mathematical expressions (19,20)directly from the CT Number of the image pixel of CT image. With an average energy in between 50 and 75keV, approximately 91% of the X-ray interactions are Compton Scatter. Therefore, the CT Numbers and CT images derive their contrast mainly from the physical properties of tissue that influence Compton Scatter (Density of tissue (gm cm^{-3}) plays an important role in discriminating property of tissue. The linear attenuation coefficient (has a linear relationship with the density of tissue. Relative electron density is the ratio of ED of the tissue to the ED of water. Thus water with a physical density of 1 and ED of $3.340X10^{15}$ $/m^3$ has a relative electron density of 1. For a CT image of a mass or lesion in the brain containing unknown materials, we calculate the relative electron density for each pixel using "relative electron density-CT Number relations curve" (figure1) provided by Matsufuji et al (20) and Watanabe (18). ED of the tissue in question can be obtained by multiplying relative electron density by $3.340X10^{23}$ cm^{-3}.

Figure 4

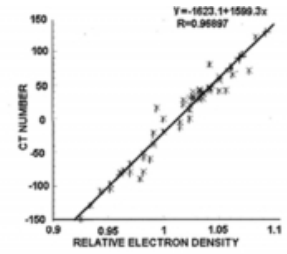

Figure1. CT Number to relative electron density conversion curve. Relative electron density is electron density(ED) relative to ED of water with density of 1. Multiplying relative electron density with $3.340X10^{23}/cm^3$ ED of the tissue is derived. ***(After Matsufuji)***

MR IMAGING, MR SPECTROSCOPY AND CT–MRI FUSION

MRI scan was performed initially on a 0.3 Tesla Hitachi ARIS II for all the cases using a quadrature head coil. ^1H MRS data were acquired using a 3 Tesla Siemens Magnetom Trio MR Scanner for the suspected pathological cases. The MR imaging sequences of these studies included axial T1 weighted (TR/TE:450/15), T2 weighted (4500/120), FLAIR (8500/120), sagittal FLAIR, and coronal T2 weighted, with a matrix size of 256 × 256 × 48 and a pixel size of 1 × 1 × 3 mm. For identifying regions of active tumor or disease the sensitivity and specificity of these images may not be optimal as the invading margin may remain invisible. Patients underwent single voxel point-resolved MR spectroscopy [PRESS] at short TE (30ms) and long TE (135ms) and MR Spectroscopic Imaging (MRSI) (PRESS) at TR/TE 3000/135) before operation to identify region of abnormal metabolism (22,23,24,25,26,27) that corresponds pathology of the tumor/mass anatomy in the colored CT and MR fusion image. This was also helpful to compare with the RI value determined from the image. We have avoided contrast study as contrast enhancement denotes abnormal blood brain barrier and the region of solid active tumor may not be enhanced. For MRSI the region of tissue studied was chosen to include most of the pathology, surrounding normal tissue avoiding bone and subcutaneous fat, and contra lateral tissue.

IMAGE PROCESSING TECHNIQUE

FUSION OF CT AND MR IMAGES - IMAGE PROCESSING TECHNIQUE

The incorporation of multiple imaging modalities is an important method for diagnosing a pathology. The method used for co-registering of MR image and CT images, along with visualization of the multimodality data and colored image, is described here. Registration of the MR images and CT scan images was performed using an automated alignment by using an interactive registration tool (a homemade software) -Color Converter©-). Color Converter provided a Image registration command to geometrically transform or registers a stack of images of a CT scan (source image) against another image of an MR (target image) using six user-defined control points. These points were tip of the nose, occiput, right and left pina of ear, vertex and chin.

The registration of the source image the target image produced a new image, the CT-MR fusion image. Then the CT-MR fusion image was colorized (figure2) It is described in detail in the colorization section. In each case, the quality of final CT-M RI registration was demonstrated by a 99% volume overlap.

COLORIZATION OF MR IMAGE

Image colorization was described below. The positions, orientations and gray scale values(out of 256 shades) of T1-weighted, inverse T2-weighted and FLAIR images as well as the digital images of the corresponding colored cross-section of brain were aligned using a rigid-body registration technique (figure 2C). Independent component analysis (ICA) basis was then applied to the registered MRI data sets of gray value of tissues as x 1, x 2 x 3 to obtain statistically independent components of corresponding color values , s 1, s 2 and s 3 (figure 2A and B)(28). This operation transformed the dataset of image pixel components (gray value) into color components (red, green, blue value) that characterized the physical features of gray and white matters, blood, CSF with their original color. Table 2 shows the gray value and corresponding color value of the tissue out of 256 shades

Figure 5

TABLE-2.Gray and corresponding color values of various tissue determined by Independent Component Analysis

Tissue	Color value Gray and color values are out of 256 shades			
	Gray value	Red value	Green value	Blue value
CSF	0 – 74	16-165	1-73	1-36
Blood	75-89	173-184	65-76	36-46
Gary matter	176-211	217-255	169-211	124-241
Mass/Tumor	90-175	184-217	76-169	46-124

A radial basis function (RBF) network, a kind of neural

network, was then used to generate the mapping function that produced correspondences between these independent components of gray value and the color components of the full color cross-section data (figure 2E). The training samples for the neural network were selected using the K-mean clustering algorithm (28) in the software Color Converter©.

Figure 6

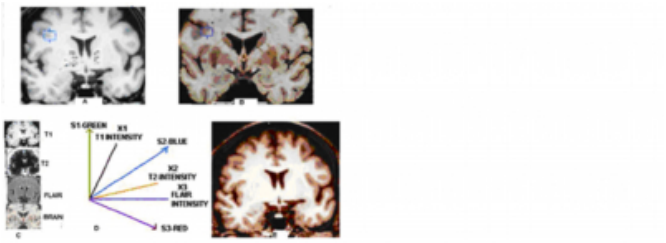

Figure 2. Coronal MR images of (A) T1 weighted image (B) digital color image of original section of brain specimen, in the same slice, plane and orientation in rigid registration to determine the gray and corresponding color value of the pixel, depicted in the back ground as X,Y pixel information. C & D Independent Component Analysis (ICA) decomposing digital image of original brain specimen to determine the red, green and blue color values of the corresponding gray value of T1, T2 weighted and FLAIR MR images, and (E) Computer generated color mapping of MR image by k-mean cluster method converting the gray scale values to corresponding color values pixel by pixel.

In image analysis the purpose of the K-mean clustering algorithm was to classify the objects in data matrix based on some selected attributes. A color shade scale was applied which determines the wavelength in nanometers from the images and in turn optical frequency of the lesion was determined from the equation f = C/, where, C = velocity of light =3 × 10^{10} cm, = wave length in cm.

DETERMINATION OF REFRACTIVE INDEX

The RI values of biopsy samples of gray matter, white matter and pathological tissue were (figure 3 F.G.H) independently determined using two methods: 1) by Abbe refractometer and 2) by ellipsometer. RI values of relatively thin tissues of 2 mm were determined by Abbe refractometer and thicker (>2mm) tissues were performed with the ellipsometer.

Figure 7

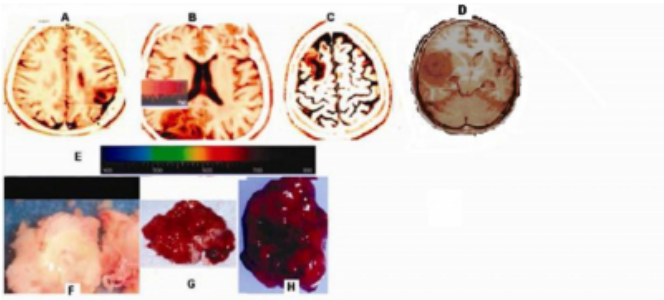

Figure 3. A) Colored MRI: low grade glioma B) Oligodendroglioma-GrII(low grade) C) Tumefactive Multiple sclerosis and D) Glioblastoma E) wavelength scale Biopsy specimen- F) Oligodendroglioma , G) Glioblastoma H) Medulloblastoma

ABBE REFRACTOMETER

Postoperative tissue specimens collected in normal saline were preserved in –80°c in the laboratory. After proper thawing of the tissue to room temperature

(20°c), a small sample was sandwiched between the illuminating prism and the refracting prism of an Abbe refractometer (Suprashes Model AAR-33).

The refracting prism of the Abbe refractometer has a high refractive index (RI= 1.75). The samples have a smaller refractive index than the refracting prism. A light source (589.3 D line) is projected through the illuminating prism. A borderline between a dark and light zones was placed over the central point of the "cross wire" of the prism by adjusting the knob of the refractometer. On a calibrating scale, the position of the borderline indicated the refractive index of the tissue. To eliminate any operator bias, five readings were taken to find the mean RI value.

DETERMINATION OF RI BY ELLIPSOMETER

For thicker biopsy material (more than 2mm) RI value and dielectric constant of thick tissue were determined with an ellipsometer, model Alpha-SE® (USA). It consisted of a laser beam (a 632.8 nm helium/neon laser), a polarizer, and a quarter wave plate, in which the sample was kept. The instrument generated polarized light, which could be set to linearly polarized light to elliptically polarized light or circularly polarized light depending on the angle of the polarizer. The beam was reflected off the layer of interest of the sample and then detected for analysis.

The angle of the polarizer and analyzer were adjusted until a minimal signal was detected. This minimum detected signal was linearly polarized, while the analyzer was set so that

only light with a polarization perpendicular to the incoming polarization was allowed to pass. The ellipsometer would then determine the dielectric constant and RI value of the biopsy material.

DETERMINATION OF GLUTATHIONE CONCENTRATION IN BIOPSY TISSUE

Identification of low concentration of GSH in ^{1}H MRS requires spectral editing techniques. Due to the difficulty in quantifying GSH by ^{1}HMRS, GSH was measured in the biopsy sample using the method of Sedlack and Lindsay (29). Cell homogenates (1×10^{6} cells) were prepared from samples of various biopsy materials using 0.15 M KCl and centrifuged at 10,000 rpm for 20 min at 4°C. Then 0.2 ml KCl and 4.8 ml EDTA (0.2M) were added to the mixture. The mixture was kept on ice for 10 minute. Deionised water and 1 ml of 5% trichloroacetic acid (TCA) were then added. The mixture was again kept on ice for 10 minute and centrifuged at 3000 rpm for 15 minute. Two ml of supernatant solution was taken, and 4 ml of 0.4 M tris buffer (pH 8.9) was added. One ml of 0.01 M 5, 5-Dithio bis (2-nitrobenzoic acid) (DTNB) solution was then added and solution vortexed thoroughly. Optical density (OD) was read (within 2 to 3 min after addition of DTNB) at 412 nm against a reagent blank.

GSH concentrations of samples were obtained by plotting OD values against a standard GSH curve (figure 4)

ESTIMATION OF TISSUE WATER CONTENT

Desiccation method was used for the estimation of water content of biopsy materials. In this method, the tissue samples were first weighed in a digital balance, then cut into small pieces and subsequently dried at 40°C to constant weight (Table3).

Concentration of water: Weight / Weight percent (w/w %) was calculated as follows:

Figure 8

$$\frac{\text{Weight of the tissue before heating - weight of the dry tissue X100}}{\text{Weight of the tissue before heating}}$$

Figure 9

TABLE-3.Various normal and pathological tissues with electron density, optical Frequency, RI values and water content

Tissue	CT NO HU	ρ Physical density +.02	Relative electron density to water	Wave Length nm	Optical frequency HZ	RI +.0.002 average	% of water
Low grade glioma	50	1.01	1.1701	720	4.40	1.432	55
Medulloblastoma	48	1.005	1.1848	650	4.3	1.441	50
Glioblastoma	52	1.001	1.2110	680	4.41	1.447	50
Metastasis	58	0.989	1.3077	625	4.76	1.4602 to 1.4833	25 to 30
Oligodendroglioma	46	0.9335	0.9358	620	4.16	1.3531	96-98
MS Tumefactive	27	0.7512	0.7477	420	7.14	1.2849	98-99
Meningioma	58 -62	1.063	0.7374	720	3.84	1.265 to 1.271	99
Wall of Solid Brain Abscess	46	1.112	1.044	560	5.35	1.3179	98
Gray matter	44	1.0045	1.06	610	4.9	1.395	80
White Matter	39	1.08	1.04	565	5.30	1.412	70
Primary Lymphoma	45	1.002	1.3054	453	6.66	1.485	35 to 40

DETERMINATION OF MASS (PHYSICAL) DENSITY

Physical density of the tissue in question was derived by measuring mass (m) and volume (v). With the help of a digital balance, the weight of the tissue specimen was determined by immersing the specimen into a water filled calibrated cylinder and noting the displaced volume. Mass density (ρ) was calculated as m/v.

RESULTS

ED values of the tissues were calculated from the CT Number-Relative electron density curve (Figure 1), while optical frequencies were determined (3.84 to 7.14Hz) from the scale of wave length matched with the color of the lesion in the image.

After the experimental determination of the RI value of gray / white matter (1.395/1.412) of the biopsy samples by ellipsometer and refractometer, resonant frequency of an electron (ω_o) bound in an atom of gray and white mater was calculated from Feynman's equation and found to be $3.74x10^{16}$ Hz.

By using color shade wavelength scale (Figure3E), wave length of gray matter was found to be 761nm (brown color) which corresponds to an optical frequency $f=0.0394X10^{16}$Hz and angular frequency of the electromagnetic wave, ω

$=2\pi f=0.2474X10^{16}$Hz. CT Number of gray matter is 44-45 HU so relative electron density was found to be 1.04 from the figure1.

This leads to ED $=1.04X3.340X10^{29}/m^3= 3.473/m^3$ $\varepsilon =$ $8.85X10^{-12}$ c^2s^2/kgm^3 and $\varepsilon =3.74x10^{16}$ Hz.

By applying Feynman's equation RI value of gray matter was found to be 1.395. Similarly the yellowish white matter with wave length of 565, optical frequency of 5.30, CT Number of 39, relative electron density of1.032 and ED 3.4402, has a RI value of 1.412.

RI values of various brain lesions calculated from the Feynman's equation were tabulated (Table 3). RI values of normal gray and white matter were found to be1.395 and 1.412 respectively which agreed well with the biopsy derived RI values. RI values of various grades of glioma ranges from 1.432 to 1.447. RI values of metastasis measures about 1.460 to 1.486 and primary lymphoma 1.465. RI values of low grade (grade-II) oligodendroglioma (1.434), muliple sclerosis (1.2849), solid brain abscess(1.317) were also determined. All these predicted RI values derived from the CT-MR fusion colored images agree fully with the biopsy determined values measured by Abbe refractometer and Ellipsometer.

Normal GSH level in white matter was found to be 1.25 mM (Sedlack and Lindsay method). GSH level was low in low grade gliomas (0.9mM), markedly low in glioblastomas (0.78to 0.82 mM), minimum in metastasis (0.76 mM), and lymphoma(0.77mM). GSH was 0.92mM in oligodendroglioma, Results are summarized in Table 4.

Figure 10

TABLE- 4. Glutathione concentration in Various Tissues

Tissue	Glutathione Level
White Matter	1.25 mM
Low Grade Glioma	1.0 mM
Medulloblastoma	0.8 mM
Glioblastoma	0.78 to 0.87 mM
Metastasis	0.76 mM
Meningioma	2.9 mM

Water is 100 % (W/W%) at a RI value of 1.333 (eg CSF). Normally, there is 80% (W/W%) water content in gray matter and 70% (W/W%) in white matter. The water content was found lower in malignant tissue as 53%(W/W%) in high grade glioma, 38% (W/W%) in lymphomas and 25 to 30 W/W% in metastasis. Water content is as high as 98(W/W%) in solid brain abscess and 98-99(w/w%) in multiple sclerosis (MS) (Table3).

DISCUSSION

RI is a function of wavelength or frequency. If the electron density and optical frequency are known, RI can be predicted from the colored CT-MR fusion image by applying the Feynman's equation mentioned above. The predicted RI values from the images and the laboratory determined RI values were in agreement. Various aspects of the results will be discussed below.

Any deviation or shift of the RI value from the normal values of gray matter (1.395) or white matter (1.412) was found to be pathological. Prediction of RI value of gray and white matter from the colored images were in agreement with the RI value determined in the laboratory by Abbe refractormer and ellipsometer.

In various pathologies, normal brown color of gray matter and yellowish white color of white matters change to reddish to dark reddish color. RI values of various pathological tissue were also determined from wavelength, optical frequency, CT Number, relative electron density and ED.

Brain lesions with an average RI value less than 1.395 ,multiple sclerosis (1.2849), or solid brain abscess near the wall (1.317). Thus, a RI value close to that of water (1.333) signifies a benign lesion. Alternatively, a lesion with a RI value greater than 1.412 was found to be malignant, such as low grade glioma (1.432), oligodendroglioma (gradeII) (1.434) medulloblastoma (1.444), glioblastoma (1.447), primary lymphoma (1.465) and metastasis (1.486). The degree of malignancy increases with increasing values of RI. The relationship between predicted versus actual values of RI is shown in (figure 5) (r-0.05 and p>0.005).

Figure 11

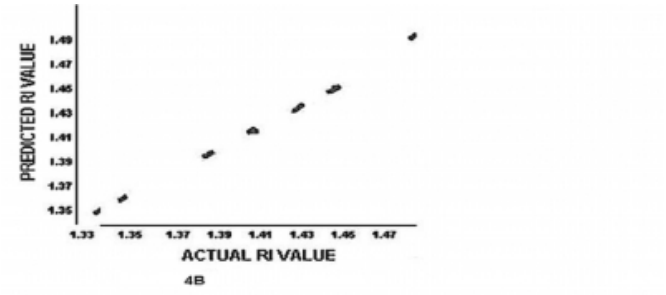

Figure 5. Graph of actual versus predicted RI value of biopsy samples and image derived RI.

A striking observation was the percentage of water content in a specimen and its relationship to RI value. Water content is 100% (w/w) at a RI of 1.333 (eg CSF). A linear relationship between RI value, water content and degree of malignancy had been found (figure 6). The lower the water content, the greater is the degree of malignancy. Water content is as high as 98 to 99% (w/w) in benign condition such as low grade oligodendroglioma, MS, and meningioma (Table3).

Malignant tumors, like glioma, glioblastoma, and metastasis show a relative decrease in antioxidant GSH levels, compared to benign tumors like low grade oligodendogliomas and meningiomas. Comparison of histopathological sections of brain tumors also suggested an inverse relationship between GSH level and grades of malignancy. A marked decrease in antioxidant GSH levels may have a role in genesis of considerable oxidative stress in brain tumors. Furthermore, the degree of decline in GSH levels indicates severity of malignancy in brain tumors. However drug (chemotherapy such as BCNU, Cis platinum) resistance glioblastoma shows increased GSH which prevents cell apoptosis (10).

In MR images, neither the gradation of the malignancy nor differentiation of tumor type can be made. Even MR spectroscopy can not distinctively discriminate between glioma tumefactive multiple sclerosis, as choline will be high and NAA will be low, resulting in a high Cho/NAA ratio. The Cho/NAA ratio also cannot differentiate between glioma and metastasis,as lactate and lipid peaks are not persistently present. RI value predicted from MR images after retrieval of true color, adds an important parameter to the accuracy of diagnosis.

In the conclusion, uniqueness of RI value to characterize tissue can be considered. It can be reliably predicted from computer-generated colored CT- MR fusion images, after applying rigid registration techniques, using electron density, and frequency of the color of the lesion. This noninvasive technique can be used prior to stereotactic biopsy, reducing risk and cost to the patient. This is a novel, noninvasive method utilizing neurophysics, neurochemistry, and neuroimaging for highly accurate diagnoses and is compatible with histopatholgy.

ACKNOWLEDGEMENT

We sincerely thank Dr Soumitra Chowdhury department of IVCCC and Dr Jaydeep Biswas Director, Chittaranjan National Cancer Institute, India for their kind support to determine glutathione level of the biopsy sample.

References

1. Saindane A, Cha S, Law M, Xue X, Knopp E, Zagzag D.Proton MR Spectroscopy of Tumefactive Demyelinating Lesions AJNR Am J Neuroradiol 2002;23:1378-1386.
2. Burtscher I, Skagerberg G, Geijer B, Englund E, Ståhlberg F, Holtås S.Proton MR Spectroscopy and Preoperative Diagnostic Accuracy: An Evaluation of Intracranial Mass Lesions Characterized by Stereotactic Biopsy Findings.AJNR Am J Neuroradiol 2000;21:84-93.
3. Alexandrov SA, Adie SG, Sampson DD. Investigating the Utility of Refractive Index tomography based on OCT.Progress in biomedical optics and imaging 2004;6:108-119.
4. Mourant JR, Fuselier T, Boyer J, Tamara M, Irving J, Bigio J.Predictions and measurement of Scattering and absorption over broad wavelength ranges in tissue phantom.Applied Optics 1997;36:949-057.
5. Kemeny G.Energy transfer mechanisms in mitochondria.ProcNatlAcadSciUSA 1974;71:3669-3671.
6. Tormos C, Chaves FJ, Garcia MJ, et al .Role of glutathione in the induction of apoptosis and c-fos and c-jun mRNAs by oxidative stress in tumor cells.Cancer letters 2004;208:103-113.
7. Babich JW.Editorial,Technetium-99m- HMPAO Retention and the Role of Glutathione :The debate continues.J Nucl Med 1991;32:1681-1683.
8. Ji L, Fu R, .Responses of glutathione system and antioxidant enzymes to exhaustive exercise and hydroperoxide.J Appl Physiol 1992;72:549-554.

9. Chaiswing L, Bourdeau-Hellera JM, Zhonga W, Oberley TD.Characterization of redox state of two human prostate carcinoma cell lines with different degrees of aggressiveness.Free Radic Biol Med 2007;43:202-215.
10. Thelwall PE, Yemin AY, Gillian TL, et al.Noninvasive In vivo Detection of Glutathione Metabolism in Tumors.Cancer Research 2005;65:10149-10153.
11. Opstad K, Provenche S, Bell B, Griffiths J, Howe F.Detection of elevated glutathione in meningiomas by quantitative in vivo 1H MRS Magn Reson Med 2003 49:632-637.
12. Giblin F.Glutathione: a vital lens antioxidant.J Ocul Pharmacol Ther 2000;16:121-135.
13. Biswas TK, Gupta A.Retrieval of true color of the internal organ of CT images and attempt to tissue characterization by refractive index : Initial experience.Indian Journal of Radiology and Imaging 2002 12:169-178.
14. Montecchia M, Montereali RM, Nichelattia E.Refractive index modification from colour centres in dielectric confining structures Optical Materials 2001;17:347-350
15. Graves EE, Prizkall A, Nelson SJ, Larson D, Verhey L.Registration of Magnetic resonance spectroscopic imaging to computed tomography for radiotherapy treatment planning.Med Phys 2001;28.
16. Feynman RP, Leighton RB, Sands M. The Feynman Lectures on Physics Volume 1; 1963. p 31.
17. Liu Y, Daum ,PH.Relationship between Refractive Index and Density and Consistency of Mixing Rules.JAerosol Science 2008; 39:974-986.
18. Watanabe Y.Derivation of linear attenuation coefficients from CT numbers for low-energy photons Phys Med Bio 1999;44:2201-2211.
19. Mustafa AA, Jackson DF.The relation between xray CT numbers and charged particle stopping powers and its significance for radiotherapy treatment planning.PhysMedBio 1983;2:169-176.
20. Matsufuji N, Tomura H, Futami Y, et al.Relationship between CT number and electrondensity,scatter angle and nuclear reaction for hardon-therapy treatment planning.Phys Med Bio 1998 43:3261-3275.
21. Rutherford RA, Pullan BR, Isherwood I.Measurement of Effective Atomic Number and Electron Density Using an EMI Scanner.Neuroradiology 1976;11 7-13.
22. Li Y, Osorio JA, Ozturk-Isik E, et al.Considerations in applying 3D PRESS H-1 brain MRSI with an eight-channel phased-array coil at 3 T.Magnetic Resonance Imaging 2006;24:1295-1302
23. Bendszus M, Warmuth-Metz M, Klein R, et al.MR Spectroscopy in Gliomatosis Cerebri AJNR Am J Neuroradiol 2000 21:375-380.
24. Sjøbakk TE, Johansen R, Bathen TF, et al.Metabolic profiling of human brain metastases using in vivo proton MR spectroscopy at 3T BMC Cancer 2007 7 141.
25. Nelson SJ.Multivoxel Magnetic Resonance Spectroscopy of Brain Tumors Molecular Cancer Therapeutics 2003;2:497-507
26. Lai PH LK, Hsu SS, Hsiao CC, et al. Pyogenic Brain Abscess , Findings from In Vivo 1.5 T and 11.7-T In Vitro Proton MR Spectroscopy AJNR Am J Neuroradiol 2005 26 279-288.
27. Huang W, Karimi S.Image-fusion of MR spectroscopic images for treatment planning of gliomas.Med Phys 2006 33:32-40.
28. Murarki S, Nakai T, Kita Y, Tsuda K.Independent component analysis of Multi Channel MRI EEE Transactions on Visualization and Computer Graphics archive 2001 vol7:265-274.
29. Sedlak J, Lindsay R.Estimation of total, protein-bound, and nonprotein sulfhydryl groups in tissue with Ellman's reagent.Anal Biochem 1968;25:192-205.

Author Information

Tapan K Biswas, M.D., PhD, D.M.R.D.
Research Scholar, Centre for Clinical Spectroscopy, Brigham and Women's Hospital, 4 Black Fan Street, Harvard Medical Institute, Boston, MA 02115.

Saadallah Ramadan, PhD
Centre for Clinical Spectroscopy, Brigham and Women's Hospital, 4 Black Fan Street, Harvard Medical Institute, Boston, MA 02115.

Samarendra Nath Ghosh, MCh
Bangur Institute of Neurosciences & Psychiatry, 52/1A, Sambhu Nath Pandit Street, Kolkata – 700025 W B, India.

Rabindra Narayan Bhattacharya, MCh
Department Of Neuroscience, AAMRI HOSPITAL, Gariahat Road Kolkata - 700 029 ,WB, India